Brain enlargement with a rostral bias in larvae from a spontaneously variant *Xenopus* female line: implications for vertebrate evolution

Ikuko Hongo[1], Chihiro Yamaguchi[2] and Harumasa Okamoto[1,*]

Department of Life Science, Faculty of Science, Gakushuin University, 1-5-1 Mejiro, Toshima-ku, Tokyo 171-8588, Japan

Present address: [1]Institute for Biomolecular Science, Gakushuin University, 1-5-1 Mejiro, Toshima-ku, Tokyo 171-8588, Japan. [2]Takasago International Corp., 5-37-1, Kamata, Ota-ku, Tokyo 144-8721, Japan.

*Author for correspondence (harumasa.okamoto@gakushuin.ac.jp)

Running title

Brain enlargement with rostral bias

Keywords

encephalisation, neocorticalisation, Spemann organiser, *chordin*, *cerberus*, *wnt11b*

Summary statement

Uncovering the developmental mechanisms of rostral-biased brain enlargement in larvae of spontaneously variant *Xenopus* females provides insights into the genetic factors that drive analogous morphogenetic transformations in vertebrate brain evolution.

ABSTRACT

Increased brain size and its rostral bias are hallmarks of vertebrate evolution, but the underlying genetic factors remain poorly understood. To gain insight into the genetic background of vertebrate brain evolution, we investigated the developmental mechanisms of brain enlargement in a subset of offspring from a spontaneously occurring variant *Xenopus* female line. Brain enlargement in the variant larvae exhibited a notable rostral bias, which could be traced back to the neural plate, the brain's primordium. At the gastrula stage, variant populations showed a dorsal-to-ventral expansion of the Spemann organiser known to induce the neural plate from the adjacent dorsal ectoderm and give it the initial rostrocaudal patterning. In fertilised variant eggs, maternal *wnt11b* mRNA, a candidate dorsalising factor, had wider distribution in the vegetal cortical cytoplasm. Specifically, its lateral spread potentially facilitated the dorsal-to-ventral expansion of *siamois* expression at the blastula stage through laterally spreading Wnt/β-catenin signalling, leading to brain enlargement via Spemann organiser expansion. Studying the spontaneous developmental variation that induces rostral-biased brain enlargement would help to uncover genetic variations that drive analogous morphogenetic transformations during vertebrate brain evolution.

INTRODUCTION

One of the most remarkable features of vertebrate evolution has been encephalisation, characterised by an increase in the ratio of brain to body size. The extent of encephalisation is quite substantial, with typical differences 10-fold and 2-3-fold between reptiles and birds, and between birds and mammals (Martin, 1981). In some species, encephalisation manifests itself primarily as neocorticalisation, an increase in the ratio of cerebral cortex to total brain size. Extensive neocorticalisation has played a prominent role in the evolution of primates, particularly humans. The human cerebral cortex is approximately 3.5 times larger in weight (de Sousa and Wood, 2007) and three times larger in number of neurons, even when compared to our closest phylogenetic relatives, chimpanzees (Herculano-Houzel and Kaas, 2011). Recent investigations have increasingly focused on the genetic variation between humans and chimpanzees (Yousaf et al., 2021), with some interesting findings. These include increased proliferation of neurogenic cells attributed to human-specific *Arhgap11b* (Florio et al., 2015; Heide et al., 2020) and increased density of longer spines attributed to human-specific *Srgap2* (Charrier et al., 2012), both observed in the human neocortex. However, the striking global differences between human and chimpanzee brain structures are not yet fully understood. Furthermore, our understanding of the mechanisms governing the overall evolution of the vertebrate brain remains incomplete. We may need a broader perspective and experimental approaches that better incorporate analyses of earlier stages of neural development.

In this study, we investigated the developmental mechanisms responsible for brain enlargement in larvae from a spontaneously occurring variant female line that we unexpectedly found in *Xenopus laevis* populations. Variant females of this line produce offspring with varying degrees of enhanced dorsal and anterior structures (dorsoanteriorisation phenotypes). Of these offspring, those with a relatively mild phenotype showed signs of brain enlargement at the larval stage. Interestingly, the spectrum of dorsoanteriorisation phenotypes, including brain enlargement, observed in the variant

offspring populations closely resembled a range of phenotypes previously produced by artificial embryonic manipulation (Kao and Elinson 1988; Scharf et al., 1989). However, the unexpected finding that spontaneously variant females produced a significantly increased number, if not all, of their offspring with enlarged brains aroused our interest in investigating this issue in detail. We hoped that the results might shed light on encephalisation and neocorticalisation in vertebrate evolution. Our rationale for this approach stems from the notion that the mechanisms governing neural development, particularly in the early stages, are fundamentally conserved across extant vertebrates, including *Xenopus*, and are therefore likely to be shared with ancestral vertebrates. A prime example of this conservation is the induction of the neural plate and its initial rostrocaudal patterning, which is mediated by specific embryonic tissues, commonly known as organisers (Houston, 2017; Stern, 2005; Wilson and Edlund, 2001). The neural plate then progressively subdivides to form the basal brain structures along the rostrocaudal axis common to vertebrates: the forebrain, midbrain, hindbrain and spinal cord (Murakami, 2017). These basal structures give rise to further subdivisions with the distinctive cellular architecture and function characteristic of different vertebrate species. For instance, in mammals, especially humans, the cerebral cortex, which comprises a rostral part of the forebrain, is prominently developed. Mutations that led to the evolutionary divergence of the brain between vertebrate species could have occurred at any stage along this continuum of neural development, but mutations at earlier stages may have had a greater impact on the divergence.

Xenopus proved advantageous for the purposes of the present study because, starting with the seminal Spemann-Mangold experiment (Spemann and Mangold, 1924), a wealth of data has been collected on the mechanisms governing early neural development in amphibians. In the present study, using whole-mount *in situ* hybridisation and serial sectioning, we have shown that the brains of *Xenopus* variant larvae with a relatively mild phenotype were enlarged from tailbud to tadpole stages.

The degree of enlargement was more pronounced towards the rostral side, particularly in the forebrain region. The rostral bias was observed as early as the formation of the brain primordium, as indicated by the expression patterns of marker genes specific for the entire neural plate or its subdivisions. Remarkably, the normally dorsally localised Spemann organiser was expanded ventrally in a large proportion of gastrulae from variant females, as evidenced by the expanded expression of *chordin* (Sasai et al., 1994) and *cerberus* (Bouwmeester et al., 1996). These genes encode proteins that are secreted by the Spemann organiser and initiate rostral neural induction. Another significant finding in the variant populations was the dorsal-to-ventral (lateral) expansion of *siamois* expression at the blastula stage. *siamois*, a transcription factor gene, is expressed dorsally and is essential for the activation of *chordin* and *cerberus* (Engleka and Kessler, 2001; Kessler, 1997). The earliest detectable change in variant embryos was the distribution pattern of maternal wnt11b mRNA. It initially localises to the vegetal cortical cytoplasm (VCC) of laid eggs and migrates dorsally following fertilisation. In the majority of eggs from variant females, maternal *wnt11b* mRNA was more diffusely distributed in the VCC compared to the control. Since Wnt11b has been implicated in *siamois* expression via the Wnt/β-catenin pathway (Brannon et al., 1997; Tao et al., 2005), lateral spread of *wnt11b* mRNA may spread *siamois* expression ventrally, leading to ventral expansion of the Spemann organiser. Our results suggest that mutations affecting a series of early intra- and intercellular signalling events can cause rostral-biased brain enlargement through expansion of the Spemann organiser in *Xenopus*.

RESULTS

Spontaneously variant females: F0 (founder) and F1 generations

Three spontaneously variant females (designated F0-1 to -3, Fig. 1A) were identified in conventional crosses with commercially available *Xenopus laevis*. A large proportion of their offspring exhibited a

range of enhanced dorsoanterior phenotypes, independent of the mating male. To facilitate our analysis, we categorised the variant larvae into three classes based on the extent of dorsoanteriorisation at stage 28/29 (panels and table in Fig. 1A): Class I with enlarged head, laterally extending cement gland, swollen trunk and shortened tail (see also Fig. 2A, B); Class II with peripherally extending cement gland, reduced trunk and rudimentary tail; Class III with cement gland surrounding the body and trunkless, tailless and cylindrically symmetrical body.

F0-1 larvae with normal morphology were reared to sexual maturity (F1 generation) to assess whether the propensity to produce larvae with enhanced dorsoanterior phenotypes was transmitted to the subsequent F1 generation. For this purpose, 5-7 randomly selected F1 females were artificially inseminated with sperm from a single normal male. In each of five such groups, the majority of F1 females produced offspring with variant phenotypes, albeit to varying degrees, whereas F1 males did not produce variant offspring when mated to normal females, confirming the primary role of maternal effects on variant phenotypes. Data from a total of 28 F1 females are summarised in Fig. 1B. They show that the propensity of F0-1 to produce the variant offspring is fairly well transmitted to the F1 female generation, although there is considerable variation in the proportion of variant phenotypes in their offspring. In the second outcross, variant females did not necessarily reproduce the same proportion of variant phenotypes as in the first cross. Similar non-reproducibility was consistently observed across successive outcrosses. The reasons for the variability between sibling females (e.g. Fig. 1B) and even at the individual level remain unknown, but we noted that the production of variant offspring tended to increase with maternal age and mating interval. In the following experiments, offspring of F0 and F1 females were collected at the desired developmental stage only when the offspring's sibling showed a high frequency of variant phenotypes at stage 29/30.

Enlargement of brain structures with rostral bias in Class I larvae

To investigate brain structures within the enlarged head of Class I larvae, we first visualised the expression of *sox2*, a pan-neural marker, at stage 29/30 by whole-mount *in situ* hybridisation (WISH) (Fig. 2). The central nervous system (CNS), apart from the spinal cord, was found to be significantly enlarged in Class I larvae compared to normal larvae (Fig. 2A'). Further examination at the level of CNS subdivisions revealed expanded expression of *bf1*, a specific marker of the forebrain and anterolateral placode, whereas *en2*, which is expressed specifically at the midbrain-hindbrain boundary, appeared to be less affected (Fig. 2B'). Similar WISH analyses of the other three Class I tailbuds yielded consistent results, confirming the rostral bias of brain enlargement in Class I tailbuds.

Brain enlargement was further investigated at the cellular level by examining nuclear stained serial cross-sections of Class I tailbuds. Each 6th section and contiguous series of sections are shown in Fig. 3 and Fig. S1, respectively. Comparison with the control revealed significantly increased cell populations in the forebrain (Fig. 3, sections s7-s25) and forebrain-derived eyes (sections s31-s43), whereas those in the hindbrain remained relatively unchanged (section s78). Assessment of midbrain cell populations was difficult because the rostral part of the neural tube bends ventrally during the relevant developmental period (Hausen and Riebesell, 1991), as confirmed by *bf1* expression in Fig. 2B'. Consequently, forebrain and midbrain regions appeared on the same cross-section at certain points (s31-s37 of normal and s31-s43 of variant brain sections). DAPI nuclear staining could not distinguish between the two regions, so the corresponding regions on these sections are labelled '1/2' ('forebrain/midbrain'). Note that the apparent ventral extension of the forebrain actually represents its rostral extension in terms of neural tube structure. Essentially the same results were obtained for the other two sets of experiments, with some variation in the degree of enlargement and the range of enlarged rostral parts in the variant brain (individual data not shown).

To follow brain development in Class I larvae, serial cross-sections were taken from tadpoles corresponding to stage 40 and stained with haematoxylin/eosin to examine changes in brain tissue architecture. Results for the most severely affected Class I tadpole are shown in Fig. 4 for each 8th section and in Fig. S2 for contiguous series of sections. Compared to a normal stage 40 tadpole, the Class I tadpole showed marked enlargement of the entire CNS from the forebrain to the spinal cord. The degree of increase in both neural cell population and ventricular size was more pronounced towards the rostral side. This synchrony between the two indices was expected because the inner surface of the ventricles consists of neuroepithelial cells, which are precursors of neuronal and glial cells. Analysis of another stage 40 equivalent Class I tadpole with a milder phenotype showed that the significant enlargement was mainly confined to the forebrain region. Taken together, the brains of the Class I variants show a rostrally biased enlargement across the larval period from stage 29/30 tailbuds to stage 40 tadpoles, although the degree and extent of enlargement varies between individuals.

Rostrally biased enlargement of neural plate structures in neurulae of variant females

We investigated the onset of brain enlargement by examining *sox2* expression. WISH analysis revealed its lateral expansion in many of the stage 13 neurulae of variant females, indicating lateral expansion of their neural plates, i.e. the brain primordium (Fig. 5A). This and subsequent experiments with embryos earlier than stage 13 were performed on all embryos grown from eggs collected from normal or variant females over a period of one to two hours, as there is minimal external difference between normal and variant embryos up to this stage of development. To quantify *sox2* expression, we measured the width of the *sox2*-positive region (d) relative to that of the embryo body (D), as illustrated in Fig. 5A. The normalised d/D values, plotted in histograms, confirmed that *sox2* expression was laterally extended in the majority of F0-1 neurulae (Fig. 5A'), albeit with

considerable inter-individual variability in this extension. The expansion of the neural plate should contribute to future brain enlargement, as confirmed in Figs. 2 to 4, since a large proportion of *sox2*-positive cells located in the central part of the neural plate give rise to neurogenic cells that populate the inner surface of the CNS ventricles (neuroepithelium) during neural tube formation. The remaining *sox2*-positive cells in the periphery are neural crest cells, the precursors of various peripheral derivatives.

We further examined the enlargement of neurogenic parts of the neural plate in sibling stage 13 neurulae. WISH analysis was performed to assess the expression of *rax*, a specific marker of the future forebrain including the prospective ocular region at stage 13 (Fig. 5B, 'd'), the specific expression of *hes7.1* at the future midbrain/hindbrain boundary (Fig. 5B, 'd_1' and 'd_2') and the expression of *foxb1* in the future posterior hindbrain region at the level of the prospective medulla (Fig. 5C, 'd'; Eagleson and Harris, 1990). For quantitative comparison, we measured the width of expression of each marker gene relative to that of the embryo body, as shown in Fig. 5B and Fig. 5C, and constructed histograms of the normalised gene expression values as for *sox2* (Figs. 5B', B'' and C'). The data showed that the expression of all three genes was laterally expanded in many of the F0-1 neurulae, but the degree of expansion appeared to differ between these genes. To confirm this difference, we defined the deviation of expression levels of each gene in variant neurulae from their normal controls (Δ) as [(mean for F0-1 neurulae – mean for control neurulae) / mean for control neurulae]. The Δ for *rax*, *hes7.1* and *foxb1* were 0.31, 0.13 and 0.08, respectively, indicating a rostral bias in the degree of expansion between the three neural plate subdivisions. Essentially the same results were obtained in the other three sets of experiments, but some variation was observed in that the deviation of *hes7.1* and *foxb1* expression tended to be smaller. This may explain the variation in the range of enlarged rostral parts we observed in stage 29/30 and 40 variant larvae. Taken together,

these results suggest that the rostrally biased brain enlargement in Class I larvae originates as early as the formation of the brain primordium.

Ventral expansion of the Spemann organiser in gastrulae of variant females

In *Xenopus laevis*, neural plate formation is initiated by anti-BMP signalling proteins such as Chordin, Noggin and Cerberus, which are secreted by the Spemann organiser and act as rostral neural inducers (Bouwmeester et al., 1996; Harland and Gerhart, 1997; Sasai et al., 1994; Stern, 2005). To investigate potential changes in the structure and function of the organiser tissue in the offspring of variant females, we analysed the expression pattern of *chordin* and *cerberus* in stage 11 gastrulae using WISH. Representative results are shown in Fig. 6A, A' for *chordin* and Fig. 6B, B' for *cerberus*. Expression of both genes appeared to be expanded ventrally in variant gastrulae (Fig. 6A, B). To quantify *chordin* expansion, the angle of the *chordin*-expressing region in the border area around the circular blastopore was measured from the centre of the blastopore ('Angle' in Fig. 6A, top right panel). The cumulative histograms in Fig. 6A' show that a large proportion of stage 11 gastrulae from F0-1 exhibited a pronounced ventral expansion of *chordin* expression, indicating a substantial expansion of the Spemann organiser tissue in the ventral direction. This was confirmed by quantitative analysis of *cerberus* expression in the same batch of gastrulae using the values of 'd' for *cerberus* expression and 'D' for embryonic body size, each term defined in Fig. 6B, top middle panel (Fig. 6B'). The considerable variability in the extent of Spemann organiser expansion inferred from Fig. 6A' and 6B' is likely to account for the phenotypic diversity observed in the larvae (Fig. 1) and neurulae (Fig. 5) of variant females.

Ventral expansion of *siamois* expression in blastulae of variant females

Activation of *chordin* and *cerberus* requires prior expression of *siamois*, which encodes a homeodomain transcription factor in *Xenopus* (Kessler, 1997). We then examined whether the expression pattern of *siamois* was altered in the offspring of variant females. In stage 9.5 late blastulae of F0-1, *siamois* was expressed dorsally near the equator, similar to the control, but in many cases the expression area expanded laterally towards the ventral side compared to the control (Fig. 7A). Cumulative histograms constructed with the values of 'd' for *siamois* expression and 'D' for embryonic body size, each term defined in Fig. 7A, quantitatively confirmed this observation (Fig. 7A'). This pattern of expanded *siamois* expression was also observed in the F1 offspring (Fig. 7A'').

We extended our analysis to the expression patterns of *chordin* and *cerberus* in stage 9.5 late blastula and stage 10 early gastrula, respectively, using the F0-1 sibling cohorts used for *siamois* analysis. Both genes were expressed in the dorsal equatorial region, but their expression expanded laterally in the majority of the offspring of the variant female (Fig. 7B, C), resembling the expression pattern of *siamois* (Fig. 7A). This expansion of *chordin* and *cerberus* was quantified as for *siamois* (Fig. 7B', C'). The considerable variability in the expansion of *chordin* (Figs. 6A' and 7B') and *cerberus* (Figs. 6B' and 7C') expression in the variant population could be attributed to the a similar variability in the expansion of the preceding *siamois* expression (Fig. 7A', A''). Collectively, these results indicate that *siamois*-expressing cells are distributed in a ventrally spreading manner in variant blastulae, leading to a ventral expansion of the Spemann organiser tissue during the gastrula stage.

Dispersed distribution of maternal *wnt11b* mRNA in the vegetal cortical cytoplasm (VCC) of variant female eggs

Siamois expression in dorsal cells requires the nuclear β-catenin/Tcf3 transcription complex in *Xenopus* (Brannon et al., 1997). Cytoplasmic β-catenin is stabilised by Wnt/β-catenin signalling to

enter the dorsal cell nucleus and form the complex. This signalling is thought to be driven by maternally derived dorsalising factors that initially localise to the VCC in newly laid eggs and translocate dorsally following fertilisation (Weaver and Kimelman, 2004). As maternal *wnt11b* mRNA is a promising candidate for such a dorsalising factor (Tao et al., 2005), we investigated whether its levels and distribution were altered in eggs from variant females. Fig. 8A shows RT-PCR analysis of mRNA levels in unfertilised eggs laid by 15 of the 28 F1 females listed in Fig. 1B. Quantified data show that *wnt11b* mRNA levels (Fig. 1B, solid circles) do not correlate with the extent of dorsoanteriorisation in the offspring of the 15 mothers examined (Fig. 1B, percentage bars), indicating that changes in the abundance of maternal *wnt11b* mRNA deposited in the laid eggs are not the primary determinant of the different dorsoanterior phenotypes in the developing offspring of the variant females.

We then compared the distribution of maternal *wnt11b* mRNA in stage 2^- embryos, identified by the appearance of the first cleavage furrow after fertilisation, from F1 and control females. They were fixed and sectioned sagittally along the future first cleavage plane to facilitate WISH analysis (Fig. 8B). As expected for a dorsalising factor, *wnt11b* mRNA was distributed in the VCC and appeared to shift from the animal-vegetal axis to a dorsal-equatorial direction in embryos from both F1 and control females (Fig. 8C). This shift may reflect cortical rotation, which moves the VCC dorsally along an animal-vegetal meridian via the microtubule-mediated transport system while retaining dorsalising factors (Gerhart, 2004; Houston, 2012, 2017; Weaver and Kimelman, 2004). For quantitative comparison, we measured the angle of rotation of the *wnt11b* mRNA-positive region (‘Angle’ in Fig. 8C, lower right panel), which was 22.0 $\pm$ 9.7 degrees and 12.8 $\pm$ 7.7 degrees in embryos from variant and control females, respectively (Fig. 8C’). The significance of these different values is uncertain as cortical rotation is a highly variable process with a range of 13-35

degrees, although it is compatible with normal development (Vincent and Gerhart, 1987). However, it could be argued that cortical rotation is not significantly affected in fertilised variant eggs.

Of particular interest in Fig. 8C is that *wnt11b* mRNA appears to be more widely distributed in the VCC compared to controls. To quantify this dispersion, we measured the width of the *wnt11b* mRNA-positive region (d_1 and d_1') relative to that of the embryo body (D), as shown in Fig. 8C, upper right panel. Histograms of normalised (d_1 + d_1')/2D values confirmed that *wnt11b* mRNA was more dispersed along the direction of d_1 measurement in many of the variant female embryos (Fig. 8C''). When measuring the degree of inward dispersion (d_2 and d_2' in Fig. 8C, upper right panel), histograms of normalised (d_2 + d_2')/2D values showed that *wnt11b* mRNA was also more inwardly dispersed in many of the variant female embryos (Fig. 8C'''). Furthermore, a similar analysis of lateral distribution ((d_3 + d_3')/2D, each term defined in Fig. 8D, upper panel) showed a more dispersed lateral distribution of *wnt11b* mRNA in many of the variant female embryos (Fig. 8D'). Taken together, these results indicate that *wnt11b* mRNA is dispersed almost omnidirectionally in stage 2^- variant embryos. Lateral spreading is of particular interest, as it may facilitate the dorsal-to-ventral (lateral) expansion of *siamois* expression at the blastula stage through laterally spreading Wnt/β-catenin signalling. The variability in the degree of lateral spreading of *wnt11b* mRNA in the variant population (Fig. 8D') may explain the variability in laterally expanded *siamois* expression in the variant blastulae (Fig. 7A', A''). These experiments were repeated with stage 2^- embryos from the other two variant females with essentially the same results.

In conclusion, a range of enhanced dorsoanterior phenotypes observed in the offspring of a spontaneously variant female line of *Xenopus*, including rostrally biased brain enlargement, can be attributed to cascading variations in intra- and intercellular signalling events initiated very early in development.

DISCUSSION

Enlargement of brain structures due to Spemann organiser expansion

We have elucidated the occurrence of a spontaneously variant female line within *Xenopus laevis* populations that produces offspring with varying degrees of enhanced dorsoanterior phenotypes (Fig. 1, Class I~III). Detailed analysis of variant larvae with a relatively mild phenotype (Class I) revealed that they have an enlarged brain with a rostral bias, while maintaining the overall basic tissue architecture (Figs. 2 to 4). The characteristic brain enlargement can be traced back to the neurula stage (Fig. 5), when the Spemann organiser has induced and begun to pattern the neural plate, i.e. the brain primordium. Since we have also shown that the Spemann organiser is expanded to quite different extents in the variants (Fig. 6), it is plausible that the brain enlargement observed in a population of variant larvae (Class I) is a consequence of a modest expansion of the Spemann organiser. Several lines of experimental evidence support this notion of a causal relationship between organiser tissue size and brain morphology, as discussed below.

A range of enhanced dorsoanterior phenotypes similar to those observed in this study (Fig. 1A), including Class I-like phenotypes, were produced by exposing 32- to 128-cell stage embryos to 0.3 M LiCl for 10-12 min (Kao and Elinson, 1988) or by exposing fertilised eggs to 30-70% D_2O for a few minutes during the first third of the first cleavage (Scharf et al., 1989). Li treatment broadly activates the Wnt/β-catenin pathway by inhibiting GSK-3β activity in the pathway, leading to enhanced dorsalisation in developing embryos (Hedgepeth et al., 1997; Klein and Melton, 1996), whereas D_2O treatment disrupts the normally unidirectional microtubule assembly, which has been suggested to expand the distribution of dorsalising factors ventrally (Scharf et al., 1989). In both cases, the resulting enhancement of dorsal and anterior structures has been attributed to an increase of Spemann organiser tissue. Indeed, our own experiments showed that D_2O treatment of normal fertilised eggs caused a ventral expansion of *chordin* expression similar to that observed in the

variant female offspring (Fig. S3A, compare with Fig. 6A'), confirming the D_2O-induced ventral expansion of the Spemann organiser. In addition, many D_2O-treated neurulae showed expanded expression of the pan-neural marker *sox2* (Fig. S3B, C) and rostral neural markers such as *bf1* (Fig. S3B, C), *emx1* and *fez* (Fig. S3C).

Experiments using morpholino oligomers (MOs) to manipulate gene expression have also supported a causal link between organiser size and brain morphology. Injection of ONT1-MO (Inomata et al., 2008) or ADMP-MO (Reversade and de Robertis, 2005) at the 4-cell stage induced a Class I-like phenotype. In MO-injected gastrulae, the organiser region was expanded ventrally. This is expected since ONT1 and ADMP normally act as fine-tuning ventralising factors in the dorsal embryonic region by increasing BMP signalling. Taken together, these previous and our present results suggest that brain enlargement in Class I larvae is most likely due to a modest expansion of the Spemann organiser, which could result from a limited number of genetic mutations.

cerberus-expressing cells in the anterior endomesodermal part of the Spemann organiser underlie the prospective forebrain, midbrain and rostral hindbrain regions of the gastrula dorsal ectoderm (labelled PFMH in Fig. 6B; Keller et al., 1992), suggesting a role for Cerberus in the development of a wide range of rostral areas of the brain. Indeed, secreted Cerberus, together with Chordin, prevents differentiation of the PFMH region into epidermal tissue by sequestering ectoderm-derived BMP protein from its receptor on PFMH cells. Cerberus also inhibits differentiation into mesodermal tissue by sequestering endomesoderm-derived Nodal and Wnt proteins (Piccolo et al., 1999). As a result, the PFMH is thought to differentiate autonomously into neuroectoderm with a rostral neural identity through intrinsic FGF/Ets signalling (Hongo and Okamoto, 2022). Subsequently, graded levels of caudalising factors such as FGF and Wnt secreted from the equatorial mesoderm posterior to the induced neuroectoderm give it an initial rostral-caudal pattern (Doniach et al., 1992; Hongo et al., 1999; Hongo et al., 1999; Hongo and Okamoto, 2022; Kiecker and Niehrs, 2001; Stern, 2005).

The expansion of *cerberus*- and *chordin*-expressing cells in the variant gastrulae (Fig. 6) should contribute significantly to the expansion of rostral neural structures at later stages, as was indeed observed (Figs. 2 to 5).

Noteworthy is the heterogeneous nature of the enlargement of brain subdivisions in the variants, which is progressively more intense rostrally and less pronounced caudally. This characteristic pattern was already observed at the stage of neural plate formation (Fig. 5). While the cause of the rostral bias requires further investigation, a plausible explanation is that the multiple organiser factors involved in neural plate formation do not increase in a functionally coordinated manner. If the overall effect of caudalising factors from the equatorial mesoderm remains largely unchanged in the variants, despite the fact that the dorsal part of the equatorial mesoderm corresponds to the posterior mesodermal part of the Spemann organiser, this could lead to a rostral bias in neural plate subdivision patterning. Indeed, our preliminary experiments suggest that FGF signalling from the equatorial mesodermal region does not appear to be significantly affected in variant gastrulae, as judged by the immunostaining pattern for P-MAPK, an indicator of FGF signalling activity (data not shown). However, further extensive studies would be required to evaluate this and other possible explanations.

Contribution of dispersed maternal *wnt11b* mRNA to Spemann organiser expansion

The activation of *siamois*, which is a prerequisite for the formation of the Spemann organiser in *Xenopus*, is triggered by dorsalising factors of maternal origin, commonly referred to as dorsal determinants (Weaver and Kimelman, 2004). The mRNAs for these determinants are thought to be pre-synthesised during oocyte maturation and localised in the cortical cytoplasm adjacent the vegetal pole of the fully mature oocyte. In the fertilised egg, these mRNAs, and presumably their translation products, are distributed in the egg VCC (vegetal cortical cytoplasm) and translocated from the

vegetal site towards the future dorsal equatorial region of the embryo. There they stabilise β-catenin via activation of the Wnt/β-catenin pathway, not necessarily from its upstream end, leading to activation of *siamois* at the blastula stage. Several potential dorsal determinants have been proposed, including Dishevelled (Miller et al., 1999; Weaver et al., 2003), phospho-Lrp6 (Dobrowolski and de Robertis, 2012), Huluwa (Yan et al., 2018) and Wnt11b (Tao et al., 2005). Translocation of dorsal determinants has been shown to be driven either by direct engagement with the microtubule-mediated transport system that assembles in the VCC shortly after fertilisation (Weaver and Kimelman, 2004), or by cortical rotation, which involves the movement of the entire VCC along an animal-vegetal meridian towards the future dorsal side of the embryo while retaining dorsal determinants. Notably, cortical rotation itself is also driven by the microtubule-mediated transport system (Gerhart, 2004; Houston, 2012, 2017). In this context, two non-exclusive functions of Wnt11b have been proposed. Firstly, dorsally transported Wnt11b directly activates the Wnt/β-catenin pathway by binding to the Wnt receptor, thereby stabilising β-catenin in dorsal cells (Tao et al., 2005). Secondly, Wnt11b promotes the ventral-dorsal unidirectional parallel assembly of microtubules in the VCC upon fertilisation, thereby facilitating microtubule-mediated transport of dorsal determinants to indirectly enhance Wnt/β-catenin signalling (Houston et al., 2022).

Current analyses remain inconclusive as to whether maternal Wnt11b functions through one or both of the proposed mechanisms. Experiments conducted with D_2O-treated fertilised eggs suggested that aberrant microtubule assembly promoted dorsoanteriorisation (Scharf et al., 1989). It was proposed that the precocious formation of a randomly arranged microtubule network caused the transfer of dorsal determinants to broader dorsal-to-ventral equatorial sectors, leading to enhanced dorsal and anterior structures. The reduction of cortical rotation observed concurrently was also attributed to this aberrant microtubule organisation. However, cortical rotation in fertilised eggs from variant females appeared unaffected (Fig. 8C, C'), indicating functional microtubule assembly in these eggs.

Indeed, preliminary immunostaining experiments showed no indication of precocious or random microtubule assembly in these eggs. It is more likely that dorsal determinants, including Wnt11b, are dispersed omnidirectionally in the VCC of variant eggs, as is *wnt11b* mRNA (Fig. 8), and move via microtubule arrays towards the wider dorsal-to-ventral equatorial region, with their movement controlled by dispersed Wnt11b. The dispersal of dorsal determinants is of unknown origin, but it may be related to the low viscosity in the VCC.

When dorsal determinants are dispersed in all directions, it may seem puzzling that *siamois*-expressing cells spread predominantly laterally without significant vertical spreading towards the animal pole (Fig. 7). However, this could be explained by the presence of another signalling pathway required for *siamois* expression, which acts in concert with the Wnt/β-catenin pathway but, unlike the latter, is active along the broad dorsal-ventral equatorial region of the blastula. The FGF signalling pathway is a prime candidate for such a pathway, as experiments with FGF2 MO indicate the requirement of FGF signalling for *siamois* expression (Fig. S4), and FGF signalling is normally activated throughout the equatorial region of the blastula (Schohl and Fagotto, 2002; our preliminary observation using anti-P-MAPK).

Implications for the evolution of the vertebrate brain

The evolutionary trend towards a larger cerebral cortex in vertebrates, particularly mammals, has long been recognised and is often referred to as neocorticalisation. However, it is noteworthy that brain enlargement extends beyond the cerebral cortex caudally to regions such as the cerebellum, albeit to a lesser extent (Barton, 2002). An evolutionary assessment of the increase in both mass and neuronal number per representative brain subdivision in primates compared to insectivores, which retain several 'primitive' mammalian features, shows that the degree of increase is progressively

greater towards the rostral side (neocortex > cerebellum > medulla; see Supplementary Information for quantified data and references).

The current investigation shows an apparently similar trend of rostral bias in the enlargement of brain subdivisions in the offspring of *Xenopus* variant females. We suggest that this may be a consequence of the uneven mutational expansion of the Spemann organiser. It is plausible that the rostral-biased brain enlargement observed evolutionarily in extant vertebrates is due, at least in part, to mutational events that occurred in ancestral vertebrate lineages, resulting in analogous expansion of tissues homologous to the Spemann organiser. Such mutated tissues present in extant species may include the hypoblast/anterior visceral endoderm/foregut endoderm and Hensen's node in birds and mice (Houston, 2017; Stern, 2005: Wilson and Edlund, 2001). The anterior visceral endoderm (AVE) in mouse embryos is of particular interest because it is the topological equivalent of the anterior endomesodermal part of the *Xenopus* Spemann organiser (Piccolo et al., 1999), which is known to secrete Cerberus as a rostral neural inducer (Bouwmeester et al., 1996). The mouse AVE also secretes Cerberus-like, a homologue of *Xenopus* Cerberus (Belo et al., 1997) and, like the *Xenopus* Spemann organiser, is thought to require nuclear β-catenin activity for its formation (Morkel et al., 2003). Also analogous to the *Xenopus* Spemann organiser, the AVE appears to play a fundamental role in the formation of the rostral CNS (Beddington and Robertson, 1999; Belo et al., 1997; Thomas and Beddington, 1996) and in the establishment of rostrocaudal polarity (Perea-Gómez et al., 2002). Consequently, functional variations in the AVE could induce a variety of changes in mouse brain development, possibly including rostral biased enlargement as in *Xenopus*. However, these issues do not seem to have been thoroughly investigated.

It is worth considering the potential consequences of widespread morphological mutations, such as rostral-biased brain enlargement, which may in some circumstances include lethality. Indeed, we have observed that Class I variants do not survive beyond the tadpole stage due to inappropriate

differentiation of digestive tissues. In *Xenopus*, *cerberus*-expressing cells in the anterior endomesoderm contribute to the development of the foregut, midgut and liver (Bouwmeester et al., 1996). Excessive proliferation of these cells (Fig. 6B, B') may not only affect the induction of neuroectoderm from the adjacent dorsal ectoderm, but may also affect the formation of digestive tissues. Survival of the Class I variant would require additional mutational events to counterbalance the lethal effects of overproduction of *cerberus*-expressing cells on digestive tissue differentiation. Relevant in this context is the well-known 'expensive-tissue hypothesis', which postulates a trade-off between brain enlargement and gut reduction during vertebrate evolution (Aiello and Wheeler, 1995). This co-evolution of brain and gut is evident between average mammals and primates, and is further accentuated in the case of humans and their primate relatives. This hypothesis is primarily based on metabolic considerations, while our present study provides embryological insights that support it.

MATERIALS AND METHODS

Xenopus adults and embryos

Adult female and male *Xenopus laevis* were obtained from Hamamatsu Seibutsu Kyouzai Corporation, Hamamatsu. The methods used to maintain them and to obtain embryos by natural mating were as previously described (Mitani and Okamoto, 1989). For artificial insemination, eggs were laid in 0.5 x MBS and fertilised with a sperm suspension in 0.1 x MBS. This was done at around 15°C, as lower temperatures seemed to be more favourable for obtaining a higher proportion of variant embryos. The fertilised eggs were then reared to the desired stage at 15-24°C in 0.1 x MBS. Embryos were staged according to Nieuwkoop and Farber (1967). Animals were handled in accordance with national guidelines and Gakushuin University guidelines for animal experimentation.

Histological procedures

Specimens were fixed in 2% paraformaldehyde and 1% glutaraldehyde in 50 mM phosphate buffer for 5 h. After rinsing with buffer, they were dehydrated in graded ethanol and embedded in paraffin according to the standard method. Sequential cross-sections were cut at 8 µm thickness for stage 29/30 tailbud samples and at 15 µm thickness for stage 40 tadpole samples. After mounting on glass slides, tailbud specimens were sealed for nuclear staining in 25% glycerol containing 1 µg/ml DAPI (4', 6-diamidino-2-phenylindole, dihydrochloride), 100 µg/ml DABCO (1, 4-diazabicyclo[2.2.2]octane), and 25 µg/ml *p*-phenylenediamine in 20 mM Tris-HCl (pH 8.2). Tadpole samples were stained with haematoxylin/eosin using standard procedures.

Whole-mount *in situ* hybridisation

Whole-mount *in situ* hybridisation experiments were performed as previously described (Hongo and Okamoto 2022).

Analysis of *wnt11b* expression by semi-quantitative RT-PCR

Total RNA was prepared from unfertilised eggs using the Proteinase K method (Sambrook et al. 1989). Semi-quantitative RT-PCR was performed as previously described, except that *odc* was used as an internal control instead of *ef1α* (Hongo and Okamoto 2022). Primer sequences were as follows. For *wnt11b*, F: 5’-ACAAAATGCAAGTGCCACGGAG-3' and R: 5’-ACCAACGGAGGTCTTGTTGCAC-3'. For *odc*, F: 5’-CACATGTCAAGCCAGTTC-3' and R: 5’-GCCTATACATTGATGCTG-3’.

Acknowledgements

We thank Professors Shigeo Okabe and Akihiko Takashima for critical reading of the manuscript.

Competing interests

The authors declare no competing or financial interests.

Funding

This work was supported in part by grant from MEXT*-Supported Program for the Private University Research Branding Project 2016–2020 (*Ministry of Education, Culture, Sports, Science and Technology).

References

Aiello, L. C. and Wheeler, P. (1995). The expensive-tissue hypothesis: the brain and the digestive system in human and primate evolution. *Curr. Anthropol*. **36**, 199–221. doi: 10.1086/204350

Barton, R. A. (2002). How did brains evolve? *Nature* **415**, 134–135. doi: 10.1038/415134a

Beddington, R. S. and Robertson, E. J. (1999). Axis development and early asymmetry in mammals. *Cell* **96**, 195-209.doi: 10.1016/s0092-8674(00)80560-7

Belo, J. A., Bouwmeester, T., Leyns, L., Kertesz, N., Gallo, M., Follettie, M. and de Robertis, E. M. (1997). Cerberus-like is a secreted factor with neuralizing activity expressed in the anterior primitive endoderm of the mouse gastrula. *Mech. Dev.* **68**, 45-57. doi: 10.1016/s0925-4773(97)00125-1

Bouwmeester, T., Kim, S., Sasai, Y., Lu, B. and de Robertis, E. M. (1996). Cerberus is a head inducing secreted factor expressed in the anterior endoderm of Spemann's organizer. *Nature* **382**, 595–601. doi:10.1038/382595a0

Brannon, M., Gomperts, M., Sumoy, L., Moon, R. T. and Kimelman, D. (1997). A β-catenin/XTcf-3 complex binds to the *siamois* promoter to regulate dorsal axis specification in *Xenopus*. *Genes Dev.* **11**, 2359–2370. doi: 10.1101/gad.11.18.2359

Charrier, C., Joshi, K., Coutinho-Budd, J., Kim, J. E., Lambert, N., de Marchena, J., Jin, W. L., Vanderhaeghen, P., Ghosh, A., Sassa, T. and Polleux, F. (2012). Inhibition of SRGAP2 function by its human-specific paralogs induces neoteny during spine maturation. *Cell* **149**, 923-935. doi: 10.1016/j.cell.2012.03.034

De Sousa, A. and Woods, B. (2007). The hominin fossil record and the emergence of the modern human central nervous system. In *Evolution of Nervous Systems: A Comprehensive Reference* **4** (ed. T.M. Preuss and J.H. Kaas), pp.291-336. Academic Press. doi: 10.1016/b0-12-370878-8/00018-5

Dobrowolski, R. and de Robertis, E. M. (2012). Endocytic control of growth factor signalling: multivesicular bodies as signalling organelles. *Nat. Rev. Mol. Cell Bio.* **13**, 53-60. doi: 10.1038/nrm3244

Doniach, T., Phillips, C.R. and Gerhart, J.C. (1992). Planar induction of anteroposterior pattern in the developing central nervous system of Xenopus laevis. Science 257, 542–545. https://doi.org/10.1126/science.1636091

Eagleson, G. W. and Harris, W. A. (1990). Mapping of the presumptive brain regions in the neural plate of *Xenopus laevis*. *J. Neurobiol.* **21**, 427-440. doi: 10.1002/neu.480210305

Engleka, M. J. and Kessler, D. S. (2001). Siamois cooperates with TGFbeta signals to induce the complete function of the Spemann-Mangold organizer. *Int. J. Dev. Biol.* **45**, 241–250. doi: 10.1387/ijdb.11291853

Florio, M., Albert, M., Taverna, E., Namba, T., Brandl, H., Lewitus, E., Haffner, C., Sykes, A., Wong, F. K., Peters, J., et al. (2015). Human-specific gene *ARHGAP11B* promotes basal progenitor amplification and neocortex expansion. *Science* **347**, 1465–1470. doi: 10.1126/science.aaa1975

Gerhart, J. (2004). Symmetry breaking in the egg of Xenopus laevis. In *Gastrulation: From Cells to Embryo* (ed. C.D. Stern), pp. 341-351. Cold Spring Harbor: CSHLpress.

Harland, R. and Gerhart, J. (1997). Formation and function of Spemann's organizer. *Annu. Rev. Cell Dev. Biol*. **13**, 611–667. doi: 10.1146/annurev.cellbio.13.1.611

Hausen, P. and Riebesell, M. (1991). *The Early Development of Xenopus Laevis: An Atlas of the Histology*. Spring-Verlag.

Hedgepeth, C. M., Conrad, L .J., Zhang, J., Huang, H. C., Lee, V. M. and Klein, P. S. (1997). Activation of the Wnt signaling pathway: A molecular mechanism for lithium action. *Dev. Biol.* **185**, 82–91. doi:10.1006/dbio.1997.8552

Heide, M., Haffner, C., Murayama, A., Kurotaki, Y., Shinohara, H., Okano, H., Sasaki, E. and Huttner, W. B. (2020). Human-specific *ARHGAP11B* increases size and folding of primate neocortex in the fetal marmoset. *Science* **369**, 546–550. doi: 10.1126/science.abb2401

Herculano-Houzel, S. and Kaas, J. H. (2011). Gorilla and orangutan brains conform to the primate cellular scaling rules: Implications for human evolution. *Brain Behav. Evol.* **77**, 33–44. doi: 10.1159/000322729

Hongo, I., Kengaku, M. and Okamoto, H. (1999). FGF signaling and the anterior neural induction in *Xenopus*. *Dev*. *Biol*. **216**, 561–581. doi: 10.1006/ dbio.1999.9515

Hongo, I. and Okamoto, H. (2022). FGF/MAPK/Ets signaling in *Xenopus* ectoderm contributes to neural induction and patterning in an autonomous and paracrine manner, respectively. *Cells Dev*. **170**, 1-20. doi: 10.1016/j.cdev.2022.203769

Houston, D. W. (2012). Cortical rotation and messenger RNA localization in *Xenopus* axis formation. *Wiley Interdiscip*. *Rev. Dev. Biol.* **1**, 371-388. doi: 10.1002/wdev.29

Houston, D. W. (2017). Vertebrate axial patterning: from egg to asymmetry. In *Vertebrate Development*: *Maternal to Zygotic Control* (ed. F. Pelegri, A. Sutherland and M. Danilchik), pp. 209-306. Cham: Springer.

Houston, D. W., Elliott, K. L., Coppenrath, K., Wlizla, M. and Horb, M. E. (2022). Maternal Wnt11b regulates cortical rotation during *Xenopus* axis formation: analysis of maternal-effect *wnt11b* mutants. *Development* **149**, 1-15. doi: 10.1242/dev.200552

Inomata, H., Haraguchi, T. and Sasai, Y. (2008). Robust stability of the embryonic axial pattern requires a secreted scaffold for chordin degradation. *Cell* **134**, 854-865. doi: 10.1016/j.cell.2008.07.008

Kao, K. R. and Elinson, R. P. (1988). The entire mesodermal mantle behaves as Spemann's organizer in dorsoanterior enhanced *Xenopus laevis* embryos. *Dev. Biol.* **127**, 64-77. doi: 10.1016/0012-1606(88)90189-3

Keller, R., Shih, J. and Sater, A. (1992). The cellular basis of the convergence and extension of the *Xenopus* neural plate. *Dev. Dyn.* **193**, 199-217. doi: 10.1002/aja.1001930302

Kessler, D. S. (1997). Siamois is required for formation of Spemann's organizer. *Proc. Natl. Acad. Sci. U.S.A.* **94**, 13017–13022. doi: 10.1073/pnas.94.24.13017

Klein P. S. and Melton D. A. (1996). A molecular mechanism for the effect of lithium on development. *Proc. Natl. Acad. Sci. U.S.A.* **93**, 8455–8459. doi: 10.1073/pnas.93.16.8455

Kiecker, C. and Niehrs, C. (2001). A morphogen gradient of Wnt/β-catenin signalling regulates anteroposterior neural patterning in *Xenopus*. *Development* **128**, 4189-4201. doi: 10.1242/dev.128.21.4189

Martin, R. D. (1981). Relative brain size and basal metabolic rate in terrestrial vertebrates. *Nature* **293**, 57–60. doi: 10.1038/293057a0

Miller, J. R., Rowning, B. A., Larabell, C. A., Yang-Snyder, J. A., Bates, R. L. and Moon, R. T. (1999). Establishment of the dorsal–ventral axis in *Xenopus* embryos coincides with the dorsal enrichment of dishevelled that is dependent on cortical rotation. *J. Cell Biol.* **146**, 427-438. doi: 10.1083/jcb.146.2.427

Mitani, S. and Okamoto, H. (1989). Embryonic development of *Xenopus* studied in a cell culture system with tissue-specific monoclonal antibodies. *Development* **105**, 53-59. doi: 10.1242/dev.105.1.53

Morkel, M., Huelsken, J., Wakamiya, M., Ding, J., van de Wetering, M., Clevers, H., Taketo, M. M., Behringer, R. R., Shen, M. M. and Birchmeier, W. (2003). Beta-catenin regulates Cripto- and

Wnt3-dependent gene expression programs in mouse axis and mesoderm formation. *Development* **130**, 6283-6294. doi: 10.1242/dev.00859

Murakami, Y. (2017). The origin of vertebrate brain centers. In *Brain evolution by design: from neural origin to cognitivearchitecture* (ed. S. Shigeno, Y. Murakami and T. Nomura). Tokyo, Japan: Springer Japan.

Nieuwkoop, P. D. and Faber, J. (1967). *Normal Table of Xenopus laevis (Daudin): A Systematical and Chronological Survey of the Development from the Fertilized Egg Till the End of Metamorphosis*. North-Holland Publishing Company. Amsterdam.

Perea-Gómez, A., Vella, F. D. J., Shawlot, W., Oulad-Abdelghani, M., Chazaud, C., Meno, C., Pfister, V., Chen, L., Robertson, E., Hamada, H. et al. (2002). Nodal antagonists in the anterior visceral endoderm prevent the formation of multiple primitive streaks. *Dev. Cell* **3**, 745-756. doi: 10.1016/s1534-5807(02)00321-0

Piccolo, S., Agius, E., Leyns, L., Bhattacharyya, S., Grunz, H., Bouwmeester, T. and de Robertis, E. M. (1999). The head inducer Cerberus is a multifunctional antagonist of Nodal, BMP and Wnt signals. *Nature* **397**, 707-710. doi: 10.1038/17820

Reversade, B. and de Robertis, E. M. (2005). Regulation of ADMP and BMP2/4/7 at opposite embryonic poles generates a self-regulating morphogenetic field. *Cell* **123**, 1147-1160. doi: 10.1016/j.cell.2005.08.047

Reversade, B., Kuroda, H., Lee, H., Mays, A. and De Robertis, E.M. (2005). Depletion of Bmp2, Bmp4, Bmp7 and Spemann organizer signals induces massive brain formation in *Xenopus* embryos. *Development* **132**, 3381–3392. doi: 10.1242/dev.01901

Sambrook, J., Fritsch, E. F. and Maniatis, T. (1989). *Molecular Cloning, second ed*. **1**, pp. 7.16-7.17. New York: Cold Spring Harbor Laboratory Press.

Sasai, Y., Lu, B., Steinbeisser, H., Geissert, D., Gont, L. K. and de Robertis, E. M. (1994). Xenopus *chordin*: a novel dorsalizing factor activated by organizer-specific homeobox genes. *Cell* **79**, 779–790. doi: 10.1016/0092-8674(94)90068-x

Scharf, S. R., Rowning, B., Wu, M. and Gerhart J. C. (1989). Hyperdorsoanterior embryos from *Xenopus* eggs treated with D2O. *Dev. Biol.* **134**, 175–188. doi: 10.1016/0012-1606(89)90087-0

Schohl, A. and Fagotto, F. (2002). β-catenin, MAPK and Smad signaling during early *Xenopus* development. *Development* **129**, 37–52. doi: 10.1242/dev.129.1.37

Spemann, H. and Mangold, H. (1924). Über Induktion von Embryonalanlagen durch Implantation artfremder Organisatoren. *Roux's Arch. EntwMech. Org.* **100**, 599-638.

Stern, C. D. (2005). Neural induction: old problem, new findings, yet more questions. *Development* **132**, 2007–2021. doi: 10.1242/dev.01794

Tao, Q., Yokota, C., Puck, H., Kofron, M., Birsoy, B., Yan, D., Asashima, M., Wylie, C. C., Lin, X. and Heasman, J. (2005). Maternal Wnt11 activates the canonical Wnt signaling pathway required for axis formation in *Xenopus* embryos. *Cell* **120**, 857-871. doi: 10.1016/j.cell.2005.01.013

Thomas, P. and Beddington, R. (1996). Anterior primitive endoderm may be responsible for patterning the anterior neural plate in the mouse embryo. *Curr. Biol.* **6**, 1487-1496. doi: 10.1016/s0960-9822(96)00753-1

Vincent, J. P. and Gerhart, J. C. (1987). Subcortical rotation in *Xenopus* eggs: anearly step in embryonic axis specification. *Dev. Biol.* **123**, 526-539. doi: 10.1016/0012-1606(87)90411-8

Weaver, C. and Kimelman, D. (2004). Move it or lose it: axis specification in *Xenopus*. *Development* **131**, 3491-3499. doi: 10.1242/dev.01284

Weaver, C., Farr, G. H., Pan, W., Rowning, B. A., Wang, J., Mao, J., Wu, D., Li, L., Larabell, C. A. and Kimelman, D. (2003). GBP binds kinesin light chain and translocates during cortical rotation in *Xenopus* eggs. *Development* **130**, 5425-5436. doi: 10.1242/dev.00737

Wilson, S. I., and Edlund, T. (2001). Neural induction: toward a unifying mechanism. *Nat. Neurosci*. **4**, 1161-1168. http://doi.org/10.1038/nn747

Yan, L., Chen, J., Zhu, X., Sun, J., Wu, X., Shen, W., Zhang, W., Tao, Q. and Meng, A. (2018). Maternal Huluwa dictates the embryonic body axis through β-catenin in vertebrates. *Science* **362**, eaat1045. doi: 10.1126/science.aat1045

Yousaf, A., Liu, J., Ye, S. and Chen, H. (2021). Current progress in evolutionary comparative genomics of great apes. *Front. Genet.* **12**, 1-7. doi: 10.3389/fgene.2021.657468

Figure legends

Fig. 1. Genealogy of spontaneously variant females of *Xenopus laevis*.

(A) Morphology of F0-1 larvae classified at stage 29/30. The table shows the proportions of each class in larvae from F0-1 to -3. n is the total number of larvae examined in a mating.

(B) The proportions of each class in larvae from F1-1 to -28 (coloured bars). The solid circles on the bars show the levels of *wnt11b* mRNA in unfertilised eggs of the respective F1 females, quantified from the data in Fig. 8A.

Fig. 2. Enlargement of brain structures in Class I larvae.

(A, B) Morphology of normal and Class I larvae at stage 29/30 used for WISH analysis in (A') and (B'). The top, middle and bottom panels in (A) and (B) show lateral, dorsal and ventral views, respectively. Scale bar: 1 mm.

(A') Expression of *sox2* in normal and Class I larvae. The arrangement of the images is the same as in (A).

(B') Expression of *bf1* (red asterisk) and *en2* (light blue asterisk) in normal and Class I larvae. Red boxed areas in (B) are magnified.

Fig. 3. Serial cross-sections through the head of normal and Class I tailbud larvae at stage 29/30.

Serial cross-sections were taken from normal and Class I larvae shown in bright field at upper left, scale bar: 1 mm. The part of the head indicated by the bidirectional arrow in the lateral view was sectioned at 8μm and the resulting serial sections were stained with DAPI. Every 6th section from section 7 (s7) to section 43 (s43) and a typical section at some distance (s78) are shown for normal (upper row) and Class I (lower row) larvae. The tissues of interest in the sections are indicated by the

numbers given to each tissue at the top of Fig. 3. Specifically, Forebrain (1), Midbrain (2) and Hindbrain (3) are outlined with yellow dotted lines. Scale bar: 0.25mm.

Fig. 4. Serial cross-sections through the head of normal and Class I tadpoles at stage 40.

Serial cross-sections were taken from normal and Class I larvae shown in bright field at upper left, scale bar: 1 mm. The part of the head indicated by the bidirectional arrow in the dorsal view was cross-sectioned at 15μm and the resulting serial sections were stained with H/E. The tissues of interest in the sections are indicated by the numbers assigned to each tissue at the top of Fig. 4. The neural tissues are indicated by a red number. Specifically, Forebrain (1), Midbrain (2) and Spinal cord (8) are outlined with red dotted lines. Scale bar: 0.25 mm.

Fig. 5. Enlargement of the neural plate and its subdivisions in stage 13 neurulae of variant females.

(A, B, C) Examples of *sox2* (A), *rax* and *hes7.1* (B) and *foxb1* (C) expression in stage 13 neurulae from control female (upper panels) and from F0-1 (lower panels).

(A') Histograms generated from *sox2* expression data. Abscissa is d/D value (% of embryo width). Mean $\pm$ SD for control and F0-1 neurulae are 62.6 $\pm$ 3.8 and 86.2 $\pm$ 10.2, respectively. The difference between the two groups is significant by t-test at $p = 1.6 \times 10^{-14}$.

(B', B'') Histograms generated from *rax* (B') and *hes7.1* (B'') expression data. Abscissa is d/D in (B') and $(d_1+d_2)/D$ in (B''). Mean $\pm$ SD values (% of embryo width) for control and F0-1 neurulae are 54.4 $\pm$ 6.2 and 71.0 $\pm$ 12.3 in *rax* and 61.0 $\pm$ 6.1 and 69.0 $\pm$ 10.9 in *hes7.1* expression, respectively. Differences between the two groups are significant by t-test at $p=3.0 \times 10^{-11}$ for *rax* expression and $p=8.5 \times 10^{-7}$ for *hes7.1* expression.

(C') Histograms generated from *foxb1* expression data. Abscissa is d/D value (% of embryo width). Mean ± SD for control and F0-1 neurulae are 43.2 ± 6.0 and 46.8 ± 4.7, respectively. The difference between the two groups is significant by t-test at $p=1.3 \times 10^{-3}$.

Fig. 6. Expanded expression of *chordin* and *cerberus* in gastrulae of variant females.

(A, B) Examples of *chordin* (A) and *cerberus* (B) expression in stage 11 gastrulae from control female (top panels) and those from F0-1 (lower panels). Dorsal, lateral and vegetal views are shown in the left, middle and right panels respectively. PFMH in the top middle panel indicates Prospective Forebrain, Midbrain and anterior Hindbrain region (see **DISCUSSION** for relevant descriptions).

(A') Histograms generated from *chordin* expression data. Abscissa is the value of the expression angle defined by 'Angle' in (A). Mean ± SD values (degrees) for control and F0-1 embryos are 86.1 ± 12.2 and 130.6 ± 47.3, respectively. The difference between the two groups is significant by t-test at $p=3.0 \times 10^{-25}$.

(B') Histograms generated from *cerberus* expression data. Abscissa is d/D value (% of embryo width). Mean ± SD for control and F0-1 embryos are 43.7 ± 8.3 and 62.4 ± 11.9, respectively. The difference between the two groups is significant by t-test at $p = 5.4 \times 10^{-19}$.

Fig. 7. Expanded expression of *siamois* in blastulae of variant females.

(A, B, C) Examples of *siamois* (A) and *chordin* (B) expression at stage 9.5 and *cerberus* (C) expression at stage 10 in embryos from control female (upper panels) and F0-1 (lower panels). Dorsal views are shown.

(A', A'') Histograms generated from *siamois* expression data. Blastulae from F0-1 (A') and F1-36 (A'') were used. F1-36 is a progeny of F0-1 from a different cross than the one that produced the F1 progeny listed in Fig. 1B. Abscissa is d/D value (% of embryo width). Mean ± SD for control and

F0-1 embryos are 42.8 ± 11.6 and 64.4 ± 16.8, respectively (A'), and 48.2 ± 8.0 and 77.0 ± 13.2 for control and F1-36 embryos, respectively (A''). Differences between control and variant groups are significant by t-test at $p=5.9 \times 10^{-32}$ for (A') and $p=1.8 \times 10^{-31}$ for (A'').

(B', C') Histograms generated from *chordin* (B') and *cerberus* (C') expression data. Abscissas in (B') and (C') are d/D values (% of embryo width) with each term defined in (B) and (C), respectively. Mean ± SD for control and F0-1 embryos are 44.4 ± 5.3 and 70.3 ± 10.0 for *chordin* expression and 43.3 ± 9.1 and 54.4 ± 7.1 for *cerberus* expression, respectively. The difference between control and F0-1 groups is significant by t-test at $p=1.4 \times 10^{-36}$ for *chordin* expression and $p=8.8 \times 10^{-13}$ for *cerberus* expression.

Fig. 8. Dispersion of maternal *wnt11b* mRNA in the vegetal cortical cytoplasm of variant female eggs.

(A) RT-PCR products of *wnt11b* mRNA in unfertilised eggs of females of the F1 generation. N in (F1-N) indicates the number assigned in Fig. 1B to the F1 females examined.

(B) Protocol for WISH using the bisection procedure and method for displaying stained samples in (C).

(C, D) Examples of *wnt11b* mRNA expression at stage 2^-. In (C), cut-surfaces of WISH-processed embryos from control female (upper panels) and F1-36 (lower panels) are shown in the arrangement illustrated in (B). In (D), embryos from control F1-14 (upper panels) and variant F1-1 (lower panels) were used. Vegetal views of the recombined embryos are shown.

(C') Histograms generated from the rotational shift data of *wnt11b* mRNA. Abscissa is the mean of the angles defined by 'Angle' on the pair of cut surfaces in (C), lower right panel. Mean ± SD (degrees) for control and F1-36 embryos are 12.8 ± 7.7 and 22.0 ± 9.7, respectively. The difference between the two groups is significant by t-test at $p = 1.3 \times 10^{-7}$.

(C'', C''', D') Histograms generated from the dispersion data of *wnt11b* mRNA. Abscissas are (d_1 + d_1')/2D in (C''), (d_2 + d_2')/2D in (C''') and (d_3 + d_3')/2D in (D'), respectively, with each term defined in (C), upper right panel, or (D), upper panel. Mean $\pm$ SD (% of embryo width) for control and variant F1 embryos are 56.3 $\pm$ 5.2 and 66.7 $\pm$ 5.8 for dorsoventral dispersion in (C''), 23.1 $\pm$ 4.7 and 29.1 $\pm$ 2.9 for inward dispersion in (C''') and 34.7 $\pm$ 9.3 and 59.0 $\pm$ 9.9 for lateral dispersion in (D'). Differences between control and variant F1 groups are significant by t-test at $p=2.7 \times 10^{-10}$ in (C''), $p=2.2 \times 10^{-7}$ in (C''') and $p=1.2 \times 10^{-17}$ in (D').

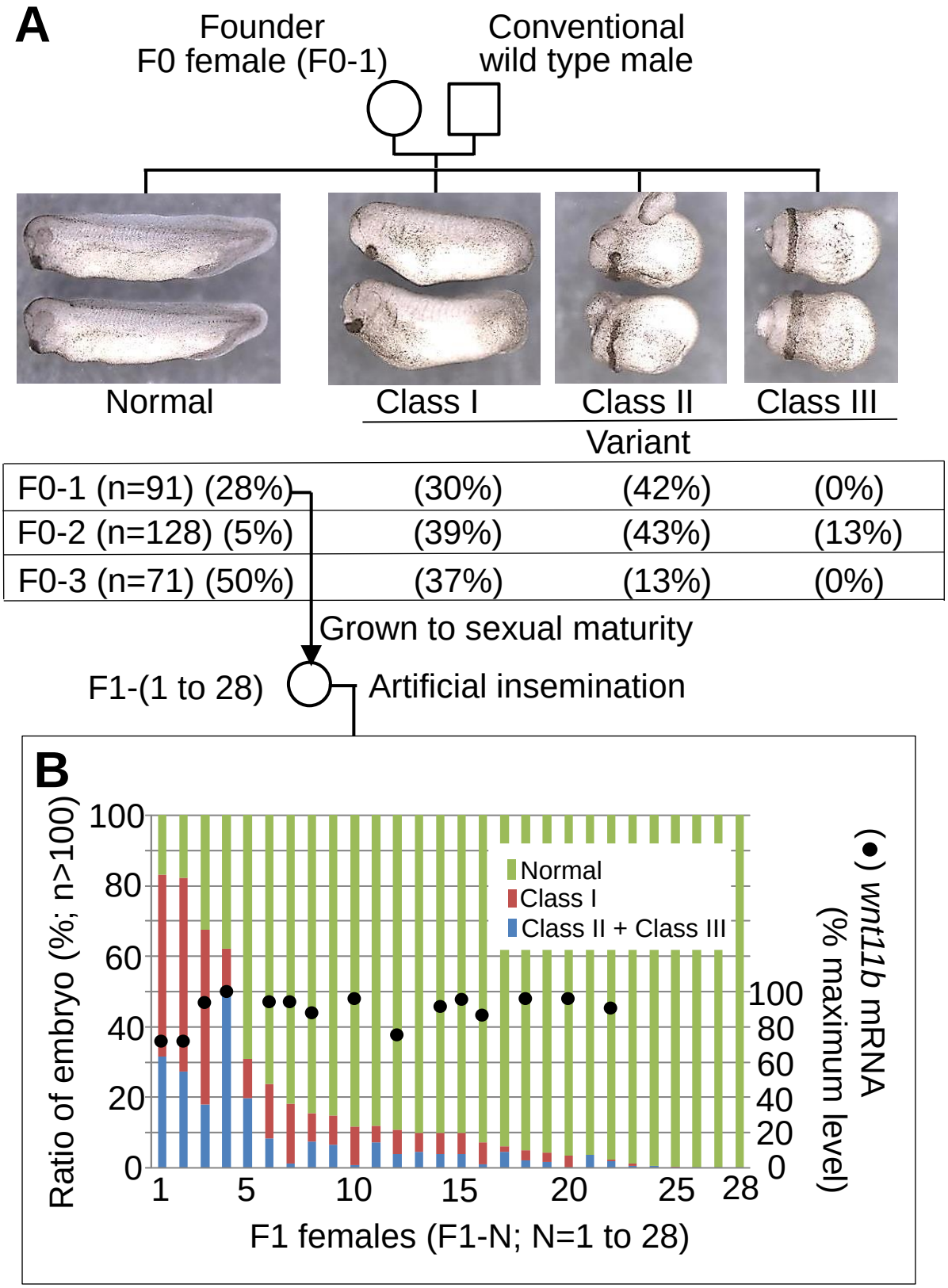
A
Founder
F0 female (F0-1)
Conventional
wild type male
Normal
Class I
Class II
Class III
Variant
F0-1 (n=91) (28%) (30%) (42%) (0%)
F0-2 (n=128) (5%) (39%) (43%) (13%)
F0-3 (n=71) (50%) (37%) (13%) (0%)
Grown to sexual maturity
F1-(1 to 28)
Artificial insemination
B
Ratio of embryo (%; n>100)
Normal
Class I
Class II + Class III
(●) wnt11b mRNA
(% maximum level)
F1 females (F1-N; N=1 to 28)

Fig. 1

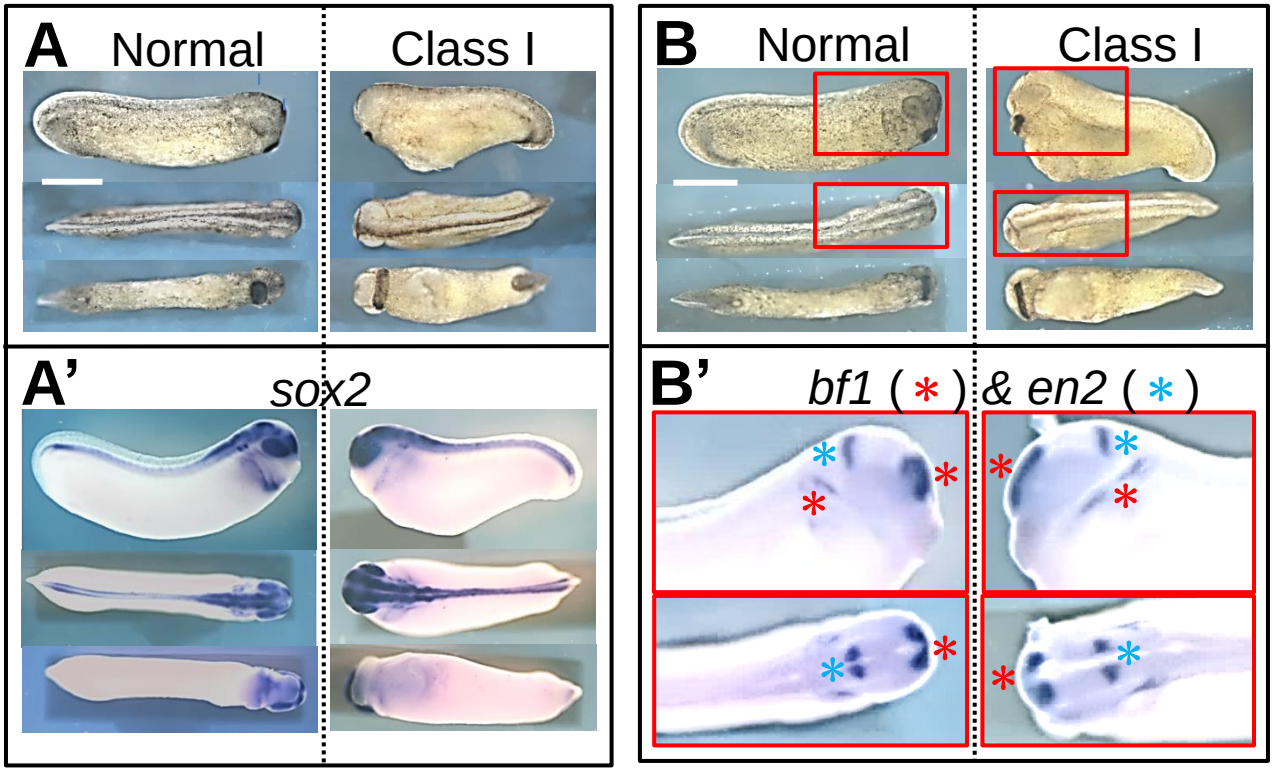

Fig. 2

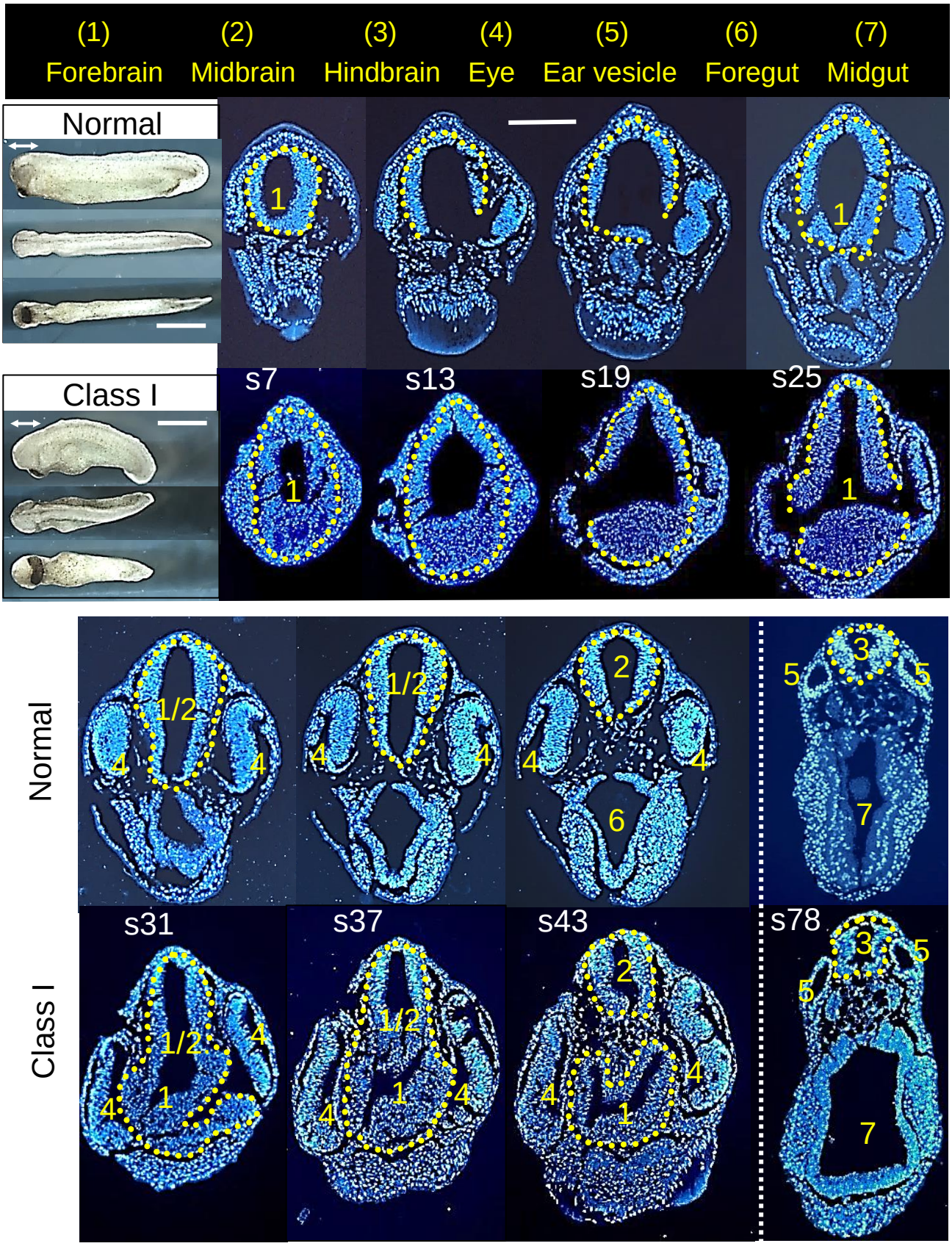
(1) Forebrain
(2) Midbrain
(3) Hindbrain
(4) Eye
(5) Ear vesicle
(6) Foregut
(7) Midgut
Normal
Class I
s7
s13
s19
s25
Normal
Class I
s31
s37
s43
s78

Fig. 3

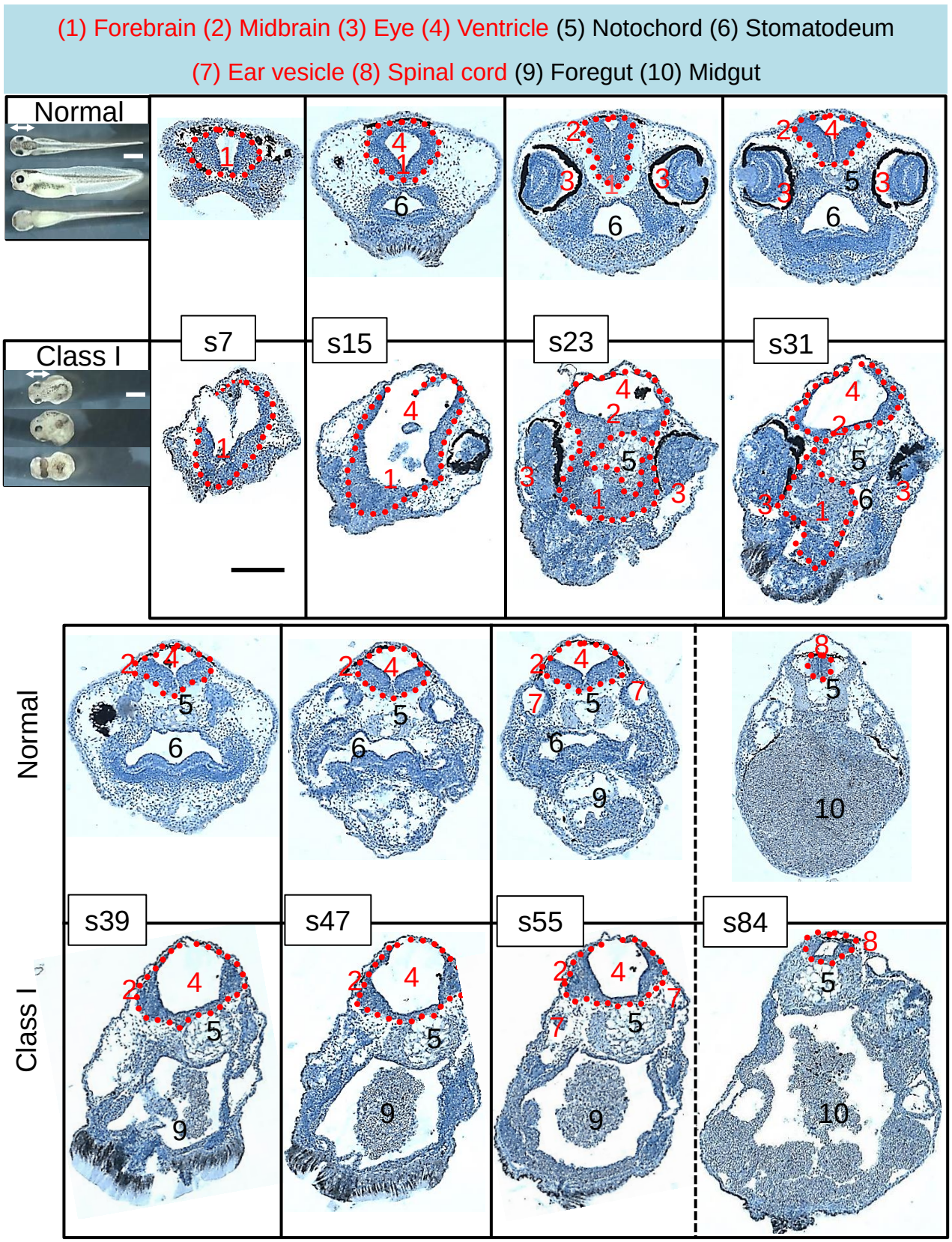
(1) Forebrain (2) Midbrain (3) Eye (4) Ventricle (5) Notochord (6) Stomatodeum
(7) Ear vesicle (8) Spinal cord (9) Foregut (10) Midgut
Normal
Class I
s7
s15
s23
s31
Normal
Class I
s39
s47
s55
s84

Fig. 4

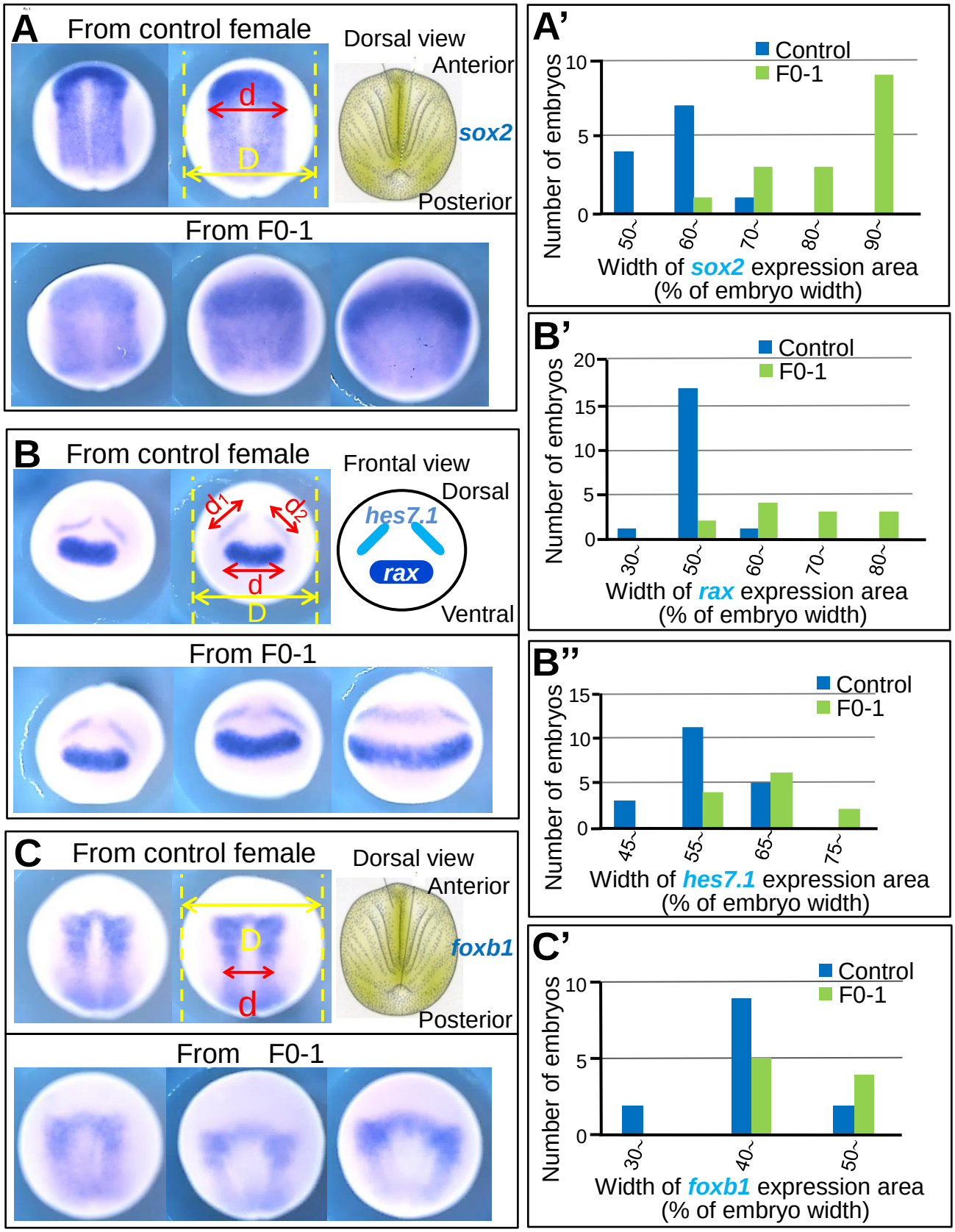
A
From control female
Dorsal view
Anterior
d
D
sox2
Posterior
From F0-1
B
From control female
Frontal view
Dorsal
d1
d2
d
D
hes7.1
rax
Ventral
From F0-1
C
From control female
Dorsal view
Anterior
D
d
foxb1
Posterior
From F0-1
A'
Control
F0-1
Number of embryos
Width of sox2 expression area
(% of embryo width)
B'
Control
F0-1
Number of embryos
Width of rax expression area
(% of embryo width)
B''
Control
F0-1
Number of embryos
Width of hes7.1 expression area
(% of embryo width)
C'
Control
F0-1
Number of embryos
Width of foxb1 expression area
(% of embryo width)

Fig. 5

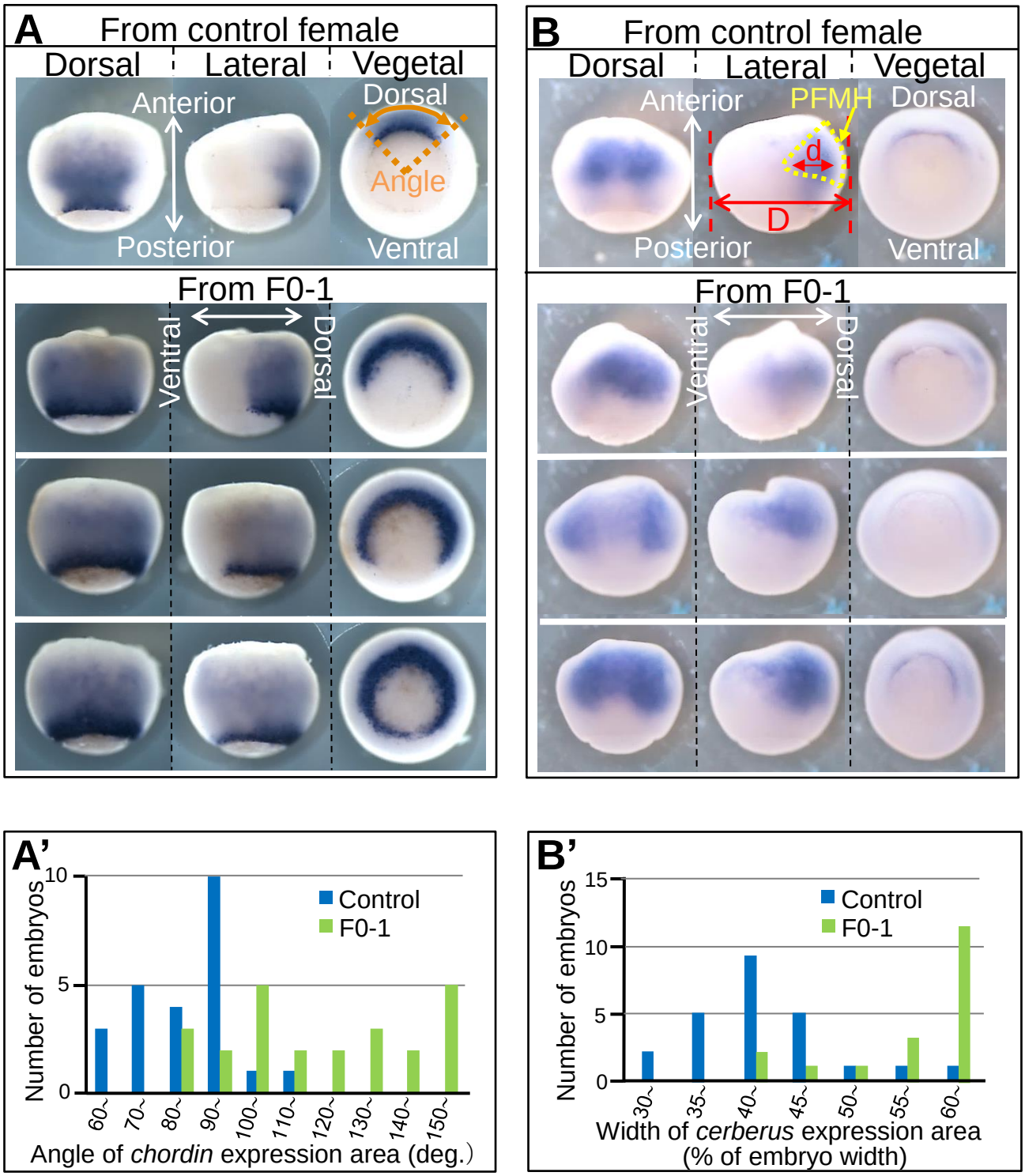
A
From control female
Dorsal
Lateral
Vegetal
Anterior
Posterior
Dorsal
Angle
Ventral
From F0-1
Ventral
Dorsal
B
From control female
Dorsal
Lateral
Vegetal
Anterior
PFMH
Dorsal
d
D
Posterior
Ventral
From F0-1
Ventral
Dorsal
A'
Number of embryos
Control
F0-1
60~
70~
80~
90~
100~
110~
120~
130~
140~
150~
Angle of chordin expression area (deg.)
B'
Number of embryos
Control
F0-1
30~
35~
40~
45~
50~
55~
60~
Width of cerberus expression area
(% of embryo width)

Fig. 6

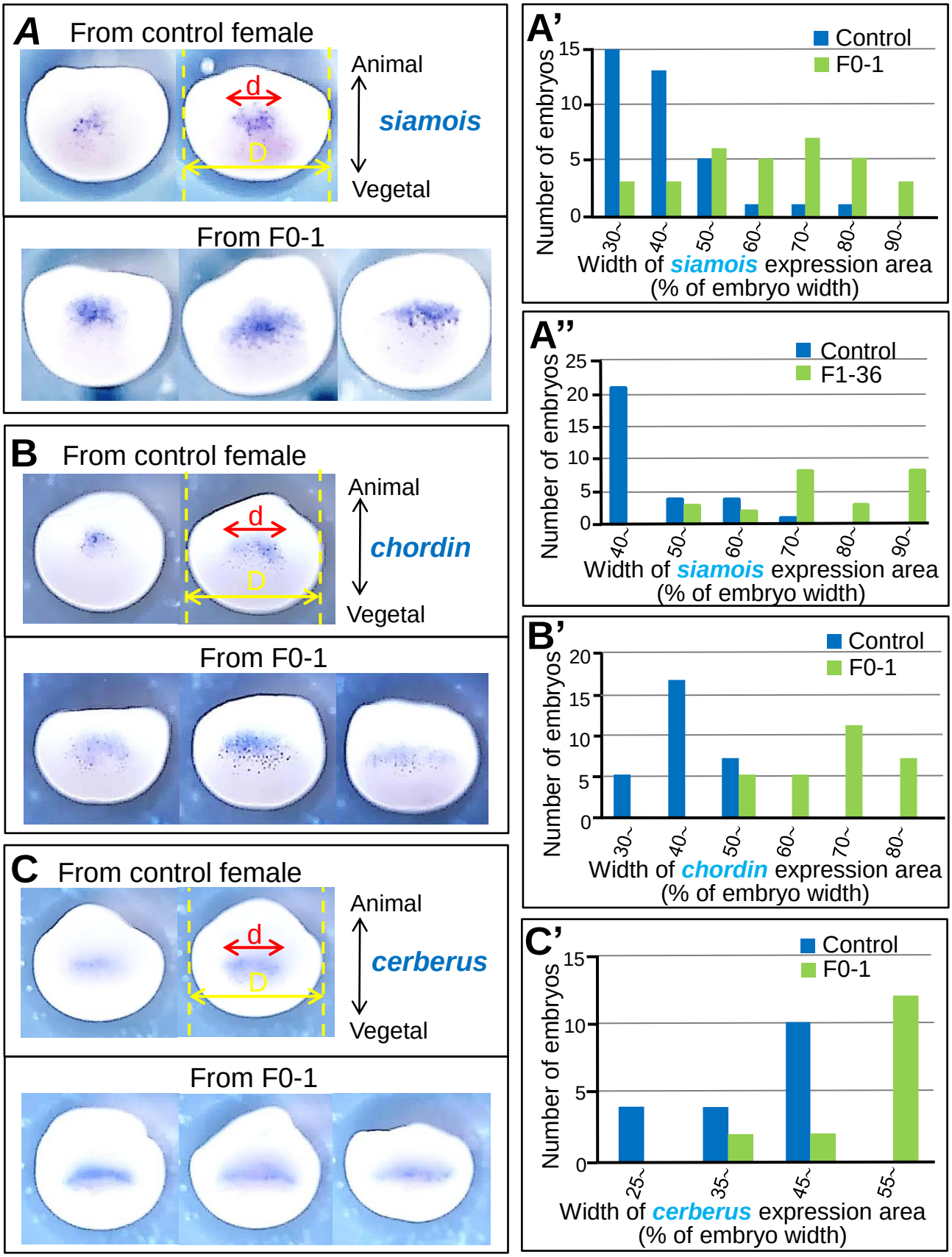
A From control female
d
D
Animal
siamois
Vegetal
From F0-1
B From control female
d
D
Animal
chordin
Vegetal
From F0-1
C From control female
d
D
Animal
cerberus
Vegetal
From F0-1
A'
Control
F0-1
Number of embryos
15
10
5
0
30~
40~
50~
60~
70~
80~
90~
Width of siamois expression area
(% of embryo width)
A''
Control
F1-36
Number of embryos
25
20
15
10
5
0
40~
50~
60~
70~
80~
90~
Width of siamois expression area
(% of embryo width)
B'
Control
F0-1
Number of embryos
20
15
10
5
0
30~
40~
50~
60~
70~
80~
Width of chordin expression area
(% of embryo width)
C'
Control
F0-1
Number of embryos
15
10
5
0
25~
35~
45~
55~
Width of cerberus expression area
(% of embryo width)

Fig. 7

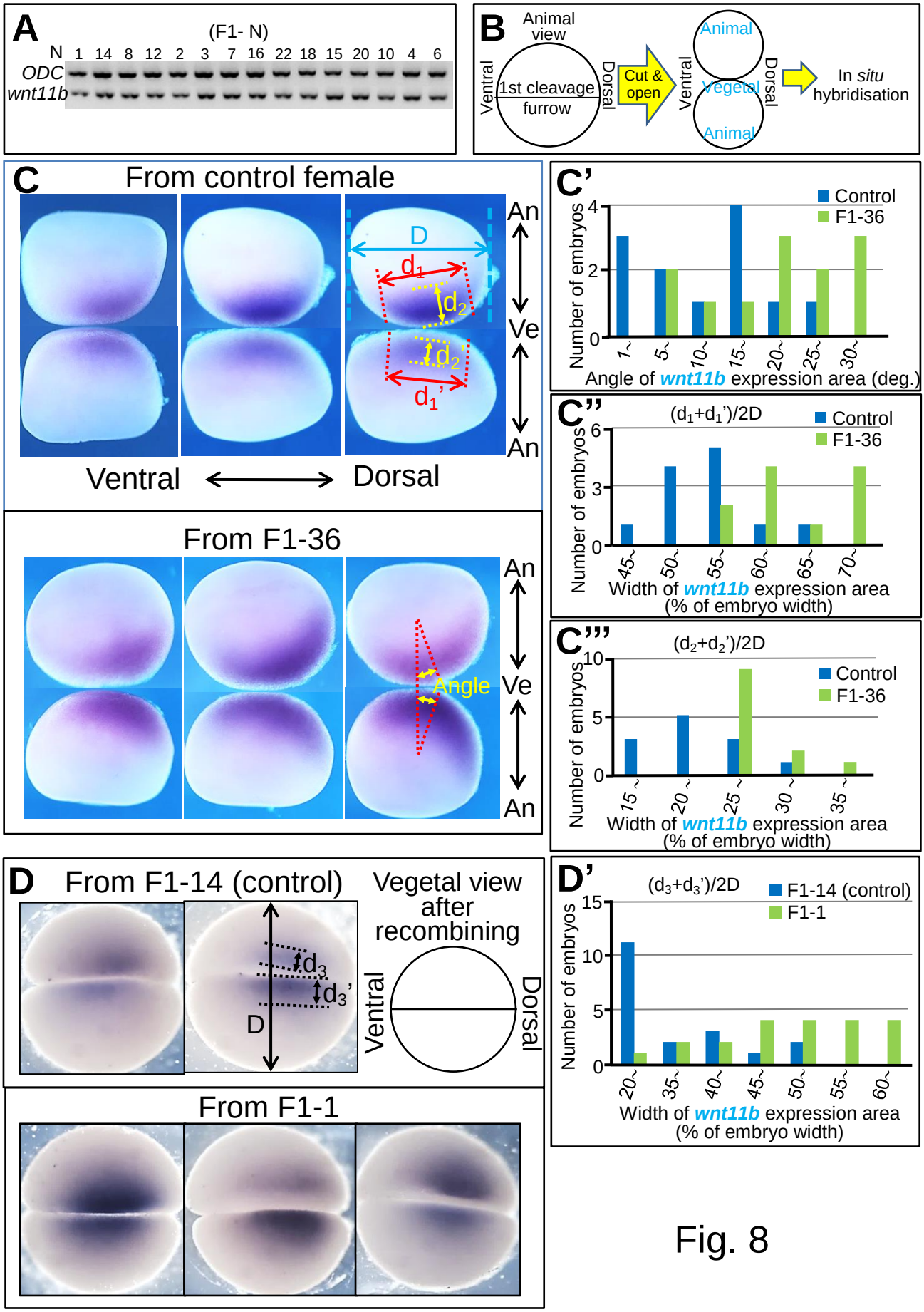
A
(F1- N)
N 1 14 8 12 2 3 7 16 22 18 15 20 10 4 6
ODC
wnt11b
B
Animal view
Ventral
1st cleavage furrow
Dorsal
Cut & open
Animal
Vegetal
Animal
In situ hybridisation
C
From control female
D
d1
d2
d1'
An
Ve
Ventral
Dorsal
From F1-36
Angle
C'
Control
F1-36
Number of embryos
Angle of wnt11b expression area (deg.)
C''
(d1+d1')/2D
Width of wnt11b expression area (% of embryo width)
C'''
(d2+d2')/2D
D
From F1-14 (control)
d3
d3'
Vegetal view after recombining
From F1-1
D'
(d3+d3')/2D
F1-14 (control)
F1-1

Fig. 8